

# Hydrothermal Synthesis and Crystal Structure of $[(\text{CH}_3\text{NH}_3)_{1.03}\text{K}_{2.97}]\text{Sb}_{12}\text{S}_{20} \cdot 1.34\text{H}_2\text{O}$

Xiqu Wang and Allan J. Jacobson<sup>1</sup>

*Department of Chemistry, University of Houston, Houston, Texas 77204-5641*

and

Friedrich Liebau

*Mineralogisches Institut der Universitaet Kiel, D-24098 Kiel, Germany*

Received November 21, 1997; in revised form May 19, 1998; accepted May 26, 1998

A novel thioantimonate(III)  $[(\text{CH}_3\text{NH}_3)_{1.03}\text{K}_{2.97}]\text{Sb}_{12}\text{S}_{20} \cdot 1.34\text{H}_2\text{O}$  was synthesized hydrothermally. It crystallizes in space group  $P\bar{1}$ , with  $a = 11.9939(7) \text{ \AA}$ ,  $b = 12.8790(8) \text{ \AA}$ ,  $c = 14.9695(9) \text{ \AA}$ ,  $\alpha = 100.033(1)^\circ$ ,  $\beta = 99.691(1)^\circ$ ,  $\gamma = 108.582(1)^\circ$ ,  $V = 2095.3(2) \text{ \AA}^3$ , and  $Z = 2$ . The structure is determined from single crystal X-ray diffraction data collected at room temperature and refined to  $R(F) = 0.037$ . In the crystal structure, each Sb(III) atom has short bonds (2.37–2.58 Å) to three S atoms. The pyramidal  $[\text{SbS}_3]$  groups share common S atoms forming two types of centrosymmetric  $[\text{Sb}_{12}\text{S}_{20}]$  rings with the same topology. These rings are interconnected by weaker Sb–S bonds (2.92–3.29 Å) into 2-dimensional layers. Adjacent layers are parallel with  $\text{K}^+$  and  $\text{CH}_3\text{NH}_3^+$  ions and  $\text{H}_2\text{O}$  molecules located between them. Variation of bond valence sums calculated for the Sb(III) cations is found to be correlated with the coordination geometry. This is interpreted as due to the stereochemical activity of their lone electron pairs. © 1998 Academic Press

## INTRODUCTION

Solventothermal methods are known to be very successful in synthesizing alkali metal thioantimonates(III) (1–10). A number of thioantimonates(III) with open framework structures have recently been synthesized under low temperature hydrothermal conditions (11–20). These new compounds have some similarities to the classical zeolite molecular sieves. However, the building principles of the thioantimonate frameworks seem more complex. Unlike the rigid tetrahedral basic building units in zeolites, the coordination polyhedra around Sb(III) are rather flexible mainly due to the stereoactivity of its lone electron pair. The Sb–S bond lengths normally vary by more than 20% within one

structure and the coordination numbers of Sb vary from 3 to 6 or even higher. The interconnection of the coordination polyhedra in thioantimonates(III) can be through sharing corners, edges and faces. However, despite the complexity shown by many known structures, structural relations between some thioantimonates have been recognized (17, 21). In a number of thioantimonates(III) the coordination environment of Sb can be considered as a hemioctahedron with different degrees of distortion. The hemioctahedra are often interconnected through edge sharing into fragments that are similar to a two atom thick (100) slice in the NaCl structure. These fragments are further interconnected into slabs, layers and frameworks. New structure types will help to better understand the general building rules for this type of compound. Here we report on the synthesis and the structure determined from single crystal X-ray data of the novel compound  $[(\text{CH}_3\text{NH}_3)_{1.03}\text{K}_{2.97}]\text{Sb}_{12}\text{S}_{20} \cdot 1.34\text{H}_2\text{O}$ .

## EXPERIMENTAL

Dark red platy crystals of  $[(\text{CH}_3\text{NH}_3)_{1.03}\text{K}_{2.97}]\text{Sb}_{12}\text{S}_{20} \cdot 1.34\text{H}_2\text{O}$  were synthesized from elemental Sb and S and an aqueous solution of KOH and  $\text{CH}_3\text{NH}_2$ . In a typical synthesis that led to a single phase product, 3 mmol Sb, 12.5 mmol S, and 3.4 mmol KOH were mixed with 2.0 ml of a 40 wt% aqueous  $\text{CH}_3\text{NH}_2$  solution. The mixture was sealed in a Teflon-lined autoclave in air and heated at  $190^\circ\text{C}$  for 4 days. The product was washed with water and ethanol, vacuum filtered and dried in air. The initial synthesis mixture is basic but it becomes more acidic as the reaction progresses. Reactions of antimony metal and sulfur under hydrothermal conditions that result in a decrease in pH have been discussed by Parise (22).

<sup>1</sup>To whom correspondence should be addressed.

Composition analysis of the crystals with a JEOL 8600 electron microprobe gave the atomic ratio (based on  $Sb = 12$ )  $K:Sb:S = 3.11:12:19.20$  which is consistent with the structure refinement results. The sulfur content determined by microprobe analysis is somewhat lower than that of the formula determined by refinement of the structure, which may be due to the instability of the crystals under the electron beam. The infrared spectrum collected on a Galaxy FTIR 5000 spectrometer using the KBr pellet method shows the presence of  $CH_3NH_3^+$  cations and water molecules in the structure (Fig. 1). Thermogravimetric analysis was carried out in nitrogen at a heating rate of  $5^\circ/\text{min}$  after initially equilibrating the sample at  $50^\circ\text{C}$  for 1 h to remove any surface water. A total weight loss of 4.3% was observed below  $315^\circ\text{C}$ , in reasonable agreement with the value calculated for loss of methylamine, water, and  $H_2S$  (3.6%). Hydrolysis of sulfide by the water present in the structure during the decomposition would result in a theoretical weight loss of 4.3% in excellent agreement with the observed value.

For single crystal X-ray data collection, a dark red plate shape crystal with approximate dimensions  $0.44 \times 0.10 \times 0.02$  mm was mounted on a glass fiber using silicon sealant. Intensities were measured on a SMART platform diffractometer equipped with a 1K CCD area detector using graphite-monochromatized  $MoK\alpha$  radiation at room temperature. A hemisphere of data (1271 frames at 5 cm detector distance) was collected using a narrow-frame method

with scan widths of  $0.30^\circ$  in  $\omega$  and an exposure time of 30 s/frame. The first 50 frames were remeasured at the end of data collection to monitor instrument and crystal stability, and the maximum correction applied on the intensities was  $<1\%$ . The data were integrated using the Siemens SAINT program (23), with the intensities corrected for Lorentz factor, polarization, air absorption, and absorption due to variation in the path length through the detector faceplate. Final cell constants were refined using 7408 reflections having  $I > 10\sigma(I)$ . An absorption correction was made by the face-indexed method using the program XPREP of the SHELXTL software package (24).

The structure was solved with direct methods and refined using SHELXTL(24). Crystallographic and refinement details are summarized in Table 1. All Sb, S, and K positions were derived by direct methods. The oxygen atom of the water molecule was located from difference maps. During refinement, the occupancies of two of the four K positions both converged at about 0.6. Weak electron density peaks were found near both positions in difference maps. These peaks were assigned to disordered water molecules and methylammonium cations which were assumed to partially substitute potassium ions. The occupancy sums of K1 and N1–C1 as well as K2 and N2–C2 were both constrained to 1 in the final refinements (Table 2). Hydrogen atoms were not included due to the large number of heavy atoms and partial occupancies of some positions.

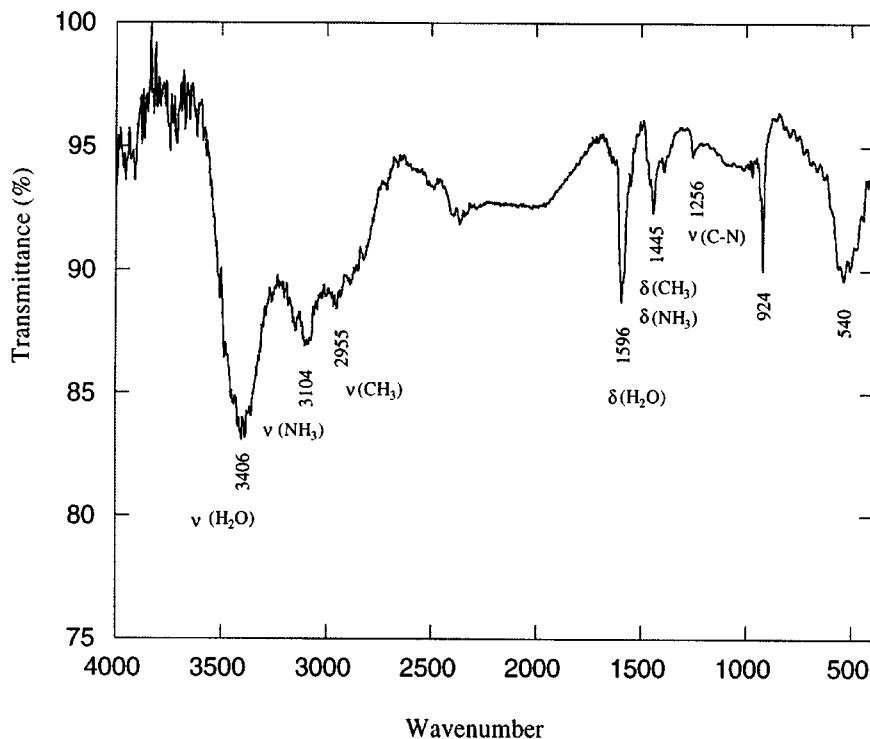


FIG. 1. Infrared spectrum of  $[(CH_3NH_3)_{1.03}K_{2.97}]Sb_{12}S_{20} \cdot 1.34H_2O$ .

**TABLE 1**  
Crystal and Structure Refinement data for  
 $[(\text{CH}_3\text{NH}_3)_{1.03}\text{K}_{2.97}]\text{Sb}_{12}\text{S}_{20} \cdot 1.34\text{H}_2\text{O}$

| Space group                            | $P\bar{1}$  |
|--|---|
| Unit cell parameters                   | $a = 11.9939(7) \text{ \AA}$ , $\alpha = 100.033(1)^\circ$<br>$b = 12.8790(8) \text{ \AA}$ , $\beta = 99.691(1)^\circ$<br>$c = 14.9695(9) \text{ \AA}$ , $\gamma = 108.582(1)^\circ$<br>$V = 2095.3(2) \text{ \AA}^3$ , $Z = 2$ |
| Crystal size                           | $0.44 \times 0.10 \times 0.02 \text{ mm}$   |
| Density (calculated)                   | $3.604 \text{ g/cm}^3$  |
| Radiation; wavelength                  | $\text{MoK}\alpha$ ; $0.71073 \text{ \AA}$  |
| Absorption coefficient                 | $8.907 \text{ mm}^{-1}$   |
| Absorption correction                  | Analytical method with 8 indexed crystal faces (SHELXTL)  |
| $2\theta$ range of data                | $3.4\text{--}54.4^\circ$  |
| Limiting indices                       | $-14 \leq h \leq 15$ , $-15 \leq k \leq 14$ ,<br>$-18 \leq l \leq 15$   |
| No. of reflections collected           | 11,293  |
| No. of independent reflections         | 7905 [ $R_{\text{int}} = 0.049$ ]   |
| Refinement method                      | Full-matrix least-squares on $F^2$ (SHELXTL)  |
| No. of data/restraints/parameters      | 7905/4/385  |
| Goodness-of-fit on $F^2$               | 1.139   |
| Final $R$ indices [ $I > 2\sigma(I)$ ] | $R(F) = 0.0367$ , $wR(F^2) = 0.0865$  |
| Final $R$ indices (all data)           | $R(F) = 0.0423$ , $wR(F^2) = 0.0910$  |
| Extinction coefficient                 | $0.00051(4)$  |
| Largest residual peak and hole         | $1.457$ and $-0.973 \text{ e \AA}^{-3}$   |

### STRUCTURE DESCRIPTION

All twelve symmetrically nonequivalent Sb atoms are each coordinated by three nearest sulfur atoms to form trigonal pyramids with Sb–S bond lengths between 2.37 and 2.58 Å and S–Sb–S angles in the range of 87.2–98.7° (Table 3). The coordination environments of Sb(1–10) are each complemented by two additional S atoms, those of Sb(11,12) each by one, with Sb–S distances between 2.92 and 3.29 Å.

If only the short Sb–S bonds (2.37–2.59 Å) are considered, the  $[\text{SbS}_3]$  trigonal pyramids are interconnected into complex rings through sharing their common S corners. The pyramids  $[\text{Sb}(1\text{--}3)\text{S}_3]$  and  $[\text{Sb}(9)\text{S}_3]$  are interconnected into elongated 8-membered rings which are centrosymmetric. Two  $[\text{Sb}(7)\text{S}_3]$  and two  $[\text{Sb}(12)\text{S}_3]$  pyramids attach to the exterior of each of these rings thus forming a loop-branched eight-membered ring of composition  $[\text{Sb}_{12}\text{S}_{20}]$  (Fig. 2). Similar 8-membered rings are formed by  $[\text{Sb}(4,6,8,10)\text{S}_3]$  pyramids which are attached by  $[\text{Sb}(5,11)\text{S}_3]$  groups. Both types of complex rings have the same composition and almost the same shape.

These complex rings are further interconnected by weaker Sb–S bonds (2.92–3.29 Å) into layers that are two atoms

**TABLE 2**  
Atomic coordinates ( $\times 10^4$ ) and Equivalent Isotropic Displacement Parameters ( $\text{\AA}^2 \times 10^3$ ) for  $[(\text{CH}_3\text{NH}_3)_{1.03}\text{K}_{2.97}]\text{Sb}_{12}\text{S}_{20} \cdot 1.34\text{H}_2\text{O}$

|        | x        | y        | z        | $U_{\text{eq}}^a$ | Occupancy |
|--------|----------|----------|----------|-------------------|-----------|
| Sb(1)  | 2891(1)  | 3234(1)  | 241(1)   | 21(1)             |           |
| Sb(2)  | 1607(1)  | 1148(1)  | 4136(1)  | 21(1)             |           |
| Sb(3)  | 716(1)   | 1334(1)  | 7864(1)  | 21(1)             |           |
| Sb(4)  | 3865(1)  | 6374(1)  | 9313(1)  | 21(1)             |           |
| Sb(5)  | 9457(1)  | 5531(1)  | 1119(1)  | 19(1)             |           |
| Sb(6)  | 6025(1)  | 8277(1)  | 1615(1)  | 20(1)             |           |
| Sb(7)  | 7279(1)  | 4081(1)  | 8282(1)  | 20(1)             |           |
| Sb(8)  | 8338(1)  | 764(1)   | 3635(1)  | 20(1)             |           |
| Sb(9)  | 7828(1)  | 6650(1)  | 7310(1)  | 22(1)             |           |
| Sb(10) | 8769(1)  | 3071(1)  | 2277(1)  | 21(1)             |           |
| Sb(11) | 5450(1)  | 8964(1)  | 4065(1)  | 25(1)             |           |
| Sb(12) | 8012(1)  | 1659(1)  | 6386(1)  | 24(1)             |           |
| S(1)   | 2146(2)  | 3865(2)  | 8518(1)  | 21(1)             |           |
| S(2)   | 4414(2)  | 5780(2)  | 1097(1)  | 22(1)             |           |
| S(3)   | 8626(2)  | 6083(2)  | 9197(1)  | 18(1)             |           |
| S(4)   | 6596(2)  | 4595(2)  | 6797(1)  | 25(1)             |           |
| S(5)   | 5617(2)  | 1529(2)  | 7646(1)  | 22(1)             |           |
| S(6)   | 3180(2)  | 365(2)   | 3797(1)  | 23(1)             |           |
| S(7)   | 9426(2)  | 9255(2)  | 7564(1)  | 26(1)             |           |
| S(8)   | 7036(2)  | 8337(2)  | 3760(1)  | 27(1)             |           |
| S(9)   | 6962(2)  | 6911(2)  | 5786(1)  | 31(1)             |           |
| S(10)  | 5015(2)  | 1573(2)  | 9909(1)  | 28(1)             |           |
| S(11)  | 6570(2)  | 992(2)   | 4193(1)  | 23(1)             |           |
| S(12)  | 964(2)   | 8007(2)  | 1932(1)  | 23(1)             |           |
| S(13)  | 3551(2)  | 2829(2)  | 1835(1)  | 28(1)             |           |
| S(14)  | 7230(2)  | 366(2)   | 1959(1)  | 23(1)             |           |
| S(15)  | 63(2)    | 5081(2)  | 2676(1)  | 23(1)             |           |
| S(16)  | 371(2)   | 8644(2)  | 4199(1)  | 29(1)             |           |
| S(17)  | 749(2)   | 7104(2)  | 6112(1)  | 25(1)             |           |
| S(18)  | 1234(2)  | 1335(2)  | 9549(1)  | 25(1)             |           |
| S(19)  | 3165(2)  | 6712(2)  | 7695(1)  | 24(1)             |           |
| S(20)  | 2001(2)  | 6469(2)  | 9731(1)  | 19(1)             |           |
| K(1)   | 8117(6)  | 4541(6)  | 5121(4)  | 65(2)             | 0.52(1)   |
| K(2)   | 8910(12) | 1150(12) | 341(12)  | 55(4)             | 0.45(2)   |
| K(3)   | 6102(2)  | 5573(2)  | 3035(2)  | 45(1)             |           |
| K(4)   | 4800(2)  | 958(2)   | 2134(2)  | 52(1)             |           |
| N(1)   | 5996(17) | 3801(16) | 4348(14) | 66(7)             | 0.48(1)   |
| C(1)   | 7298(22) | 4125(27) | 4810(19) | 79(9)             | 0.48(1)   |
| N(2)   | 8603(29) | 1209(33) | 254(28)  | 39(7)             | 0.55(2)   |
| C(2)   | 7572(22) | 486(19)  | 9478(15) | 59(6)             | 0.55(2)   |
| OW1    | 8425(6)  | 5971(6)  | 3984(5)  | 47(2)             |           |
| OW2    | 7538(17) | 9896(18) | 8795(15) | 43(8)             | 0.34(3)   |

<sup>a</sup> $U_{\text{eq}}$  is defined as one-third of the trace of the orthogonalized  $U_{ij}$  tensor. Unless otherwise stated, site occupancy equals 1.

thick. The layers are stacked parallel to the  $(\bar{2}11)$  plane (Figs. 3 and 4). The shortest Sb–S distance between layers is 3.47 Å. Neighboring layers are shifted relative to each other along the  $[120]$  direction so that the two kinds of rings are alternately stacked and outline a channel system **A** parallel to  $[100]$ . Interconnection of the rings by weaker Sb–S bonds outlines another channel system **B** that has a slightly larger channel width and is also parallel to  $[100]$  (Fig. 4).

**TABLE 3**  
**Selected Bond Lengths (Å) and Angles (deg) of [(CH<sub>3</sub>NH<sub>3</sub>)<sub>1.03</sub>**  
**K<sub>2.97</sub>]Sb<sub>12</sub>S<sub>20</sub> · 1.34H<sub>2</sub>O[Sb(1–12)S<sub>n</sub>] Polyhedra**

|                | Distances | Angles    |           |           |                     |
|----------------|-----------|-----------|-----------|-----------|---------------------|
| <b>Sb1–</b>    |           |           |           |           |                     |
| S3             | 2.463(2)  |           |           |           |                     |
| S18            | 2.516(2)  | 88.04(6)  |           |           |                     |
| S13            | 2.580(2)  | 90.76(6)  | 95.50(7)  |           |                     |
| S1             | 2.920(2)  | 86.01(6)  | 87.63(6)  | 175.43(6) |                     |
| S2             | 3.108(2)  | 78.82(6)  | 166.13(6) | 89.13(6)  | 87.08(5)            |
| Other S > 3.85 |           |           |           |           |                     |
| <b>Sb2–</b>    |           |           |           |           |                     |
| S6             | 2.487(2)  |           |           |           |                     |
| S9             | 2.510(2)  | 89.48(7)  |           |           |                     |
| S7             | 2.520(2)  | 93.65(7)  | 95.20(7)  |           |                     |
| S16            | 3.117(2)  | 79.27(6)  | 166.98(7) | 92.07(6)  |                     |
| S8             | 3.141(2)  | 85.03(6)  | 83.95(6)  | 178.43(6) | 88.52(6)            |
| Other S > 3.75 |           |           |           |           |                     |
| <b>Sb3–</b>    |           |           |           |           |                     |
| S12            | 2.466(2)  |           |           |           |                     |
| S18            | 2.494(2)  | 91.81(7)  |           |           |                     |
| S7             | 2.544(2)  | 94.15(7)  | 87.18(6)  |           |                     |
| S1             | 3.047(2)  | 81.10(6)  | 85.26(6)  | 170.93(6) |                     |
| S16            | 3.153(2)  | 78.49(6)  | 169.92(6) | 90.77(6)  | 95.81(6)            |
| Other S > 3.78 |           |           |           |           |                     |
| <b>Sb4–</b>    |           |           |           |           |                     |
| S20            | 2.455(2)  |           |           |           |                     |
| S10            | 2.508(2)  | 91.26(7)  |           |           |                     |
| S19            | 2.583(2)  | 90.53(6)  | 94.75(7)  |           |                     |
| S2             | 2.931(2)  | 86.03(6)  | 90.49(6)  | 173.80(6) |                     |
| S1             | 3.114(2)  | 79.49(6)  | 170.51(6) | 87.54(6)  | 86.76(5)            |
| Other S > 3.74 |           |           |           |           |                     |
| <b>Sb5–</b>    |           |           |           |           |                     |
| S1             | 2.400(2)  |           |           |           |                     |
| S15            | 2.543(2)  | 96.49(7)  |           |           |                     |
| S20            | 2.559(2)  | 92.92(6)  | 96.26(6)  |           |                     |
| S12            | 3.025(2)  | 82.59(6)  | 91.00(6)  | 171.86(6) |                     |
| S3             | 3.158(2)  | 81.88(6)  | 178.25(6) | 83.20(5)  | 89.43(5)            |
| Other S > 3.59 |           |           |           |           |                     |
| <b>Sb6–</b>    |           |           |           |           |                     |
| S5             | 2.472(2)  |           |           |           |                     |
| S10            | 2.480(2)  | 92.45(7)  |           |           |                     |
| S14            | 2.526(2)  | 96.16(7)  | 87.82(6)  |           |                     |
| S2             | 3.057(2)  | 82.15(6)  | 88.17(6)  | 175.57(6) |                     |
| S8             | 3.213(2)  | 76.80(6)  | 168.39(7) | 89.01(6)  | 94.56(5)            |
| Other S > 3.91 |           |           |           |           |                     |
| <b>Sb7–</b>    |           |           |           |           |                     |
| S2             | 2.414(2)  |           |           |           |                     |
| S4             | 2.509(2)  | 94.57(7)  |           |           |                     |
| S3             | 2.550(2)  | 91.99(6)  | 96.27(6)  |           |                     |
| S5             | 3.127(2)  | 81.55(6)  | 96.62(6)  | 166.00(6) |                     |
| S20            | 3.218(2)  | 80.50(6)  | 174.72(6) | 82.11(5)  | 84.56(5)            |
| Other S > 3.64 |           |           |           |           |                     |
| <b>Sb8–</b>    |           |           |           |           |                     |
| S11            | 2.487(2)  |           |           |           |                     |
| S14            | 2.514(2)  | 91.42(7)  |           |           |                     |
| S17            | 2.542(2)  | 88.94(7)  | 96.21(6)  |           |                     |
| S8             | 3.071(2)  | 80.11(6)  | 92.50(6)  | 166.18(6) |                     |
| S16            | 3.192(2)  | 85.08(6)  | 176.18(6) | 82.21(6)  | 88.42(6)            |
| S7             | 3.473(2)  | 166.01(6) | 77.18(6)  | 84.33(6)  | 108.13(5) 106.05(5) |
| Other S > 4.29 |           |           |           |           |                     |

**TABLE 3—Continued**

|   | Distances | Angles   |           |           |           |
|---|-----------|----------|-----------|-----------|-----------|
| <b>Sb9–</b>                                 |           |          |           |           |           |
| S13   | 2.437(2)  |          |           |           |           |
| S9  | 2.468(2)  | 97.59(8) |           |           |           |
| S4  | 2.490(2)  | 95.78(7) | 90.26(7)  |           |           |
| S3  | 3.111(2)  | 79.64(6) | 173.09(6) | 83.76(6)  |           |
| S7  | 3.207(2)  | 91.28(7) | 80.60(6)  | 169.14(6) | 105.69(5) |
| Other S > 3.86                              |           |          |           |           |           |
| <b>Sb10–</b>                                |           |          |           |           |           |
| S19   | 2.429(2)  |          |           |           |           |
| S17   | 2.451(2)  | 96.76(7) |           |           |           |
| S15   | 2.461(2)  | 98.68(7) | 93.43(7)  |           |           |
| S20   | 3.205(2)  | 77.56(6) | 172.76(6) | 83.12(6)  |           |
| S14   | 3.286(2)  | 84.59(6) | 80.56(6)  | 173.50(6) | 103.12(5) |
| Other S > 4.10                              |           |          |           |           |           |
| <b>Sb11–</b>                                |           |          |           |           |           |
| S8  | 2.371(2)  |          |           |           |           |
| S11   | 2.484(2)  | 95.87(7) |           |           |           |
| S5  | 2.533(2)  | 93.69(7) | 96.60(7)  |           |           |
| S6  | 3.170(2)  | 86.30(6) | 82.13(6)  | 178.72(6) |           |
| Other S > 3.72                              |           |          |           |           |           |
| <b>Sb12–</b>                                |           |          |           |           |           |
| S16   | 2.370(2)  |          |           |           |           |
| S6  | 2.481(2)  | 96.03(7) |           |           |           |
| S12   | 2.507(2)  | 94.89(7) | 94.82(7)  |           |           |
| S11   | 3.265(2)  | 85.30(6) | 80.20(6)  | 175.01(6) |           |
| Other S > 3.66                              |           |          |           |           |           |
| Other atoms                                 |           |          |           |           |           |
| K1–OW1 2.70(1) K3–OW1 2.747(8)              |           |          |           |           |           |
| S17 3.327(6) S4 3.230(3)                    |           |          |           |           |           |
| N1–C1 1.49(1) S4 3.344(6) S8 3.288(3)       |           |          |           |           |           |
| S9 3.33(2) S15 3.495(6) S2 3.350(3)         |           |          |           |           |           |
| S19 3.40(2) S17 3.625(8) S19 3.388(3)       |           |          |           |           |           |
| S4 3.51(2) S9 3.785(6) S1 3.405(3)          |           |          |           |           |           |
| Other S > 4.07 S13 3.758(3)                 |           |          |           |           |           |
| Other S > 3.99                              |           |          |           |           |           |
| C1–S4 3.23(3) K2–OW2 2.53(2) K4–OW2 2.68(2) |           |          |           |           |           |
| S17 3.55(3) S18 3.17(2) S19 3.143(3)        |           |          |           |           |           |
| S19 3.61(3) S18 3.18(2) S5 3.165(3)         |           |          |           |           |           |
| N2–C2 1.47(1) S14 3.49(2) S13 3.272(3)      |           |          |           |           |           |
| S20 3.29(4) S20 3.58(1) S14 3.278(3)        |           |          |           |           |           |
| S18 3.40(4) S7 3.64(2) S11 3.420(3)         |           |          |           |           |           |
| S14 3.41 (5) S3 3.70(2) S6 3.451(3)         |           |          |           |           |           |
| S18 3.46(4) S12 3.76(2) S10 3.587(3)        |           |          |           |           |           |
| S6 3.66 (5) Other S > 4.68 Other S > 4.15   |           |          |           |           |           |
| C2–S18 3.51(2)                              |           |          |           |           |           |
| S20 3.59(2)                                 |           |          |           |           |           |

The K<sup>+</sup> and CH<sub>3</sub>NH<sub>3</sub><sup>+</sup> cations and water molecules are located at the intersections of the channels with the inter-layer space. For both channel systems **A** and **B**, the spaces near the narrow edges of the elongated channels are occupied by K3 and K4 atoms, whereas the spaces along the channel axes are occupied by K1 and K2 which are partially substituted by the larger CH<sub>3</sub>NH<sub>3</sub><sup>+</sup> cations in a random

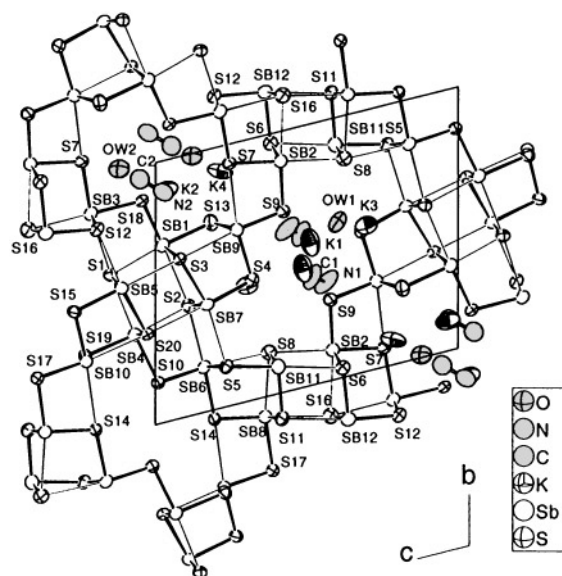


FIG. 2. A fragment of the structure of  $[(\text{CH}_3\text{NH}_3)_{1.03}\text{K}_{2.97}]\text{Sb}_{12}\text{S}_{20} \cdot 1.34\text{H}_2\text{O}$  projected along  $[100]$  showing atom labeling scheme. Thermal ellipsoids are at 75% probability. Thick and thin solid lines represent Sb-S bond lengths in the ranges 2.37–2.59 and 2.92–3.29 Å, respectively.

way. The water molecules in channel B are well ordered, while those in channel A are disordered (Fig. 4).

### DISCUSSION

Dark red crystals of  $[(\text{CH}_3\text{NH}_3)_{1.03}\text{K}_{2.97}]\text{Sb}_{12}\text{S}_{20} \cdot 1.34\text{H}_2\text{O}$  were obtained as a single phase by hydrothermal

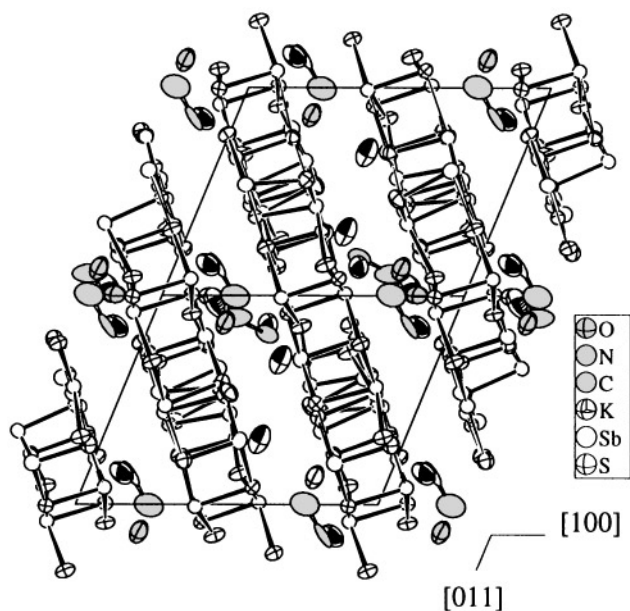


FIG. 3. Projection along  $[01\bar{1}]$  of the structure of  $[(\text{CH}_3\text{NH}_3)_{1.03}\text{K}_{2.97}]\text{Sb}_{12}\text{S}_{20} \cdot 1.34\text{H}_2\text{O}$ .

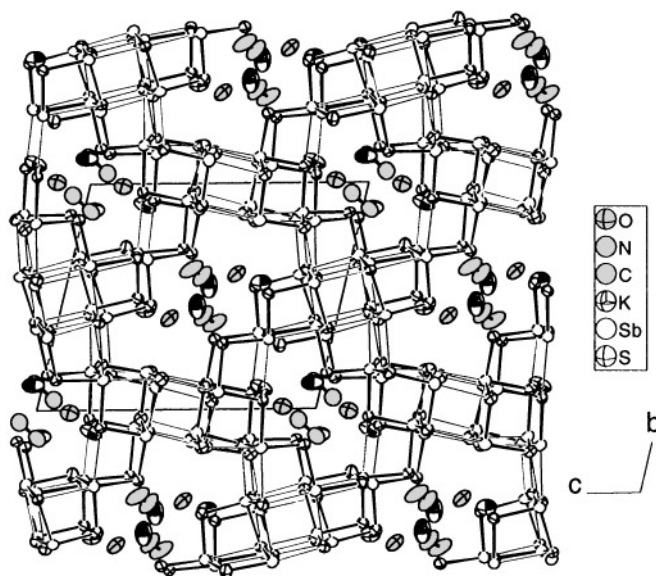


FIG. 4. Projection along  $[100]$  of the structure of  $[(\text{CH}_3\text{NH}_3)_{1.03}\text{K}_{2.97}]\text{Sb}_{12}\text{S}_{20} \cdot 1.34\text{H}_2\text{O}$ . Axis of channel A is located at the origin of the unit cell and axis of B at the middle of the unit cell.

reaction of Sb and S in the presence of KOH and  $\text{CH}_3\text{NH}_2$ . The composition was determined from the X-ray structure refinement and confirmed by electron microprobe and thermogravimetric analysis data. The infrared spectrum confirms the presence of methylammonium cations and water molecules in the structure.

Bond valence sums (BVS) calculated using the parameters from Brese and O'Keeffe (25) for the Sb atoms range from 2.85 to 3.26 v.u., indicating all the Sb atoms are formally trivalent. It has been noted previously (26,27) that a large deviation of the calculated BVS from the integer oxidation numbers for lone pair cations such as Sb(III) are correlated to the stereoactivity of the lone electron pairs (LEP) of the cations. In Fig. 5 for each  $[\text{SbS}_{4,5}]$  polyhedron the BVS is plotted against a parameter  $|\Phi|$  calculated according to Wang and Liebau (27), which is considered a measure of the stereoactivity of the lone electron pairs. Large  $|\Phi|$  values indicate strong deviation of the spatial distribution of the LEP from spherical symmetry. A good correlation between BVS and  $|\Phi|$  can be seen for Sb(1–10) that have similar hemioctahedral coordination. Sb(11–12) have quarter-octahedral coordination, which might be the reason why they deviate considerably from the trend defined by Sb(1–10).

Sb(9–12) have higher  $|\Phi|$  values, indicating stronger  $sp^3$  character of their LEP (26). The LEP of these Sb(III) cations should be on the opposite side of the three shortest Sb-S bonds of each  $[\text{SbS}_3]$  pyramid. As can be seen from Fig. 2, the LEP of Sb(9–12) should be inclined toward the interior of the  $[100]$  channels, where repulsion with S anions and

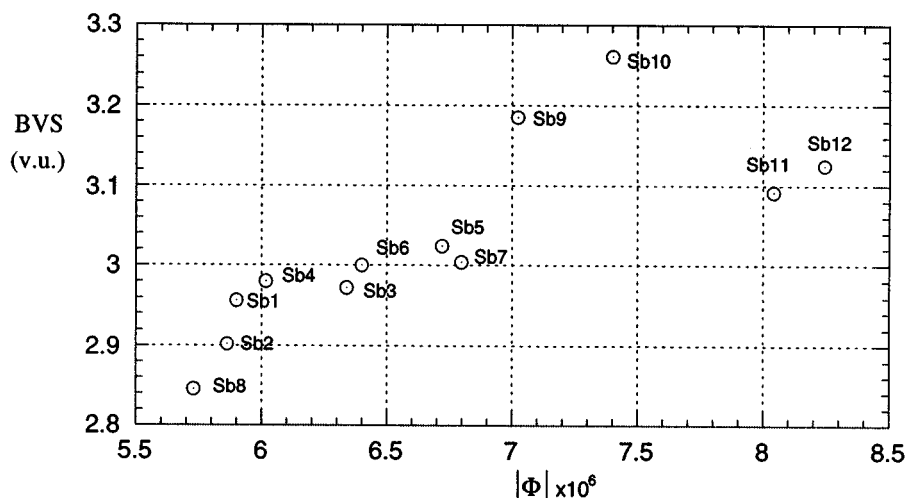


FIG. 5. Plot of bond valence sums calculated for Sb atoms against the parameter  $|\Phi|$ .  $|\Phi|$  is the length of vector  $\Phi = -\sum \phi_{ij}$  where  $\phi_{ij}$  is a vector pointing from  $Sb_i$  to the coordinating  $S_j$  at distance  $D_{ij}$  and the length of  $\phi_{ij}$  is  $\exp(-D_{ij}/0.2)$ . The summation is over all coordinating S atoms of a polyhedron (27).

other LEP are weaker, and therefore, stronger deviation of the LEP from spherical distribution around its nucleus is favored. Such deviation results in higher effective atomic valences of these cations (or overbonding as it is referred to in some literature), which are compensated by the lower effective valences (underbonding) of the neighboring cations Sb2 and Sb8, as reflected by the formal BVS values of these Sb(III) cations. Therefore, as have been noted (26), lone pair cations with the equal oxidation numbers (formal valence) may have different effective valences (bonding power) in the same structure.

The two-atom-thick layers in the title compound, shown in Fig. 6a, can be considered as derivatives of a [SbS] layer that is similar to a (100) slice of the NaCl structure. In order to form the complex anion of the composition  $Sb_3S_5$ , some of the Sb positions in a [SbS] layer are unoccupied. The layer shown in Fig. 6a is strongly distorted compared to the idealized NaCl structure scheme shown in Fig. 6b, especially near the vacant positions where the space is available for guest species. Such two-atom-thick layers can be conveniently described with two-dimensional nets. If for each node of a net, the following possible cases are symbolized by

- $\uparrow$ , Sb top, S bottom;  $\downarrow$ , Sb bottom, S top;  
 $\uparrow$ , Sb missing, S bottom;  $\downarrow$ , Sb missing, S top,

then the  $[Sb_3S_5]$  layer in the structure of  $[(CH_3NH_3)_{1.03}K_{2.97}]Sb_{12}S_{20} \cdot 1.34H_2O$ , shown in Fig. 6a and in the idealized scheme in Fig. 6b, can be represented as Fig. 6c. All infinite vertical columns are identical and neighboring columns are shifted either one or three atom positions verti-

cally relative to each other. Each column has a symmetry of the one dimensional group  $\bar{1}$  and an asymmetric unit  $\uparrow\downarrow\uparrow\downarrow$ . Similarly, each horizontal infinite row also has a symmetry line group  $\bar{1}$ . However, the rows with odd row numbers (referred to Fig. 6c) have an asymmetric unit  $\uparrow\downarrow\uparrow\downarrow\uparrow\downarrow\uparrow\downarrow$  and the rows with even row numbers are mirror images of their neighboring rows. Each row is shifted 4 atom positions to the right relative to the one above it. These two asymmetric units, each accounting for one of the two basis lines with line group symmetry  $\bar{1}$  of the net, define the layer topology shown in Fig. 6. The  $Sb_3S_5$  stoichiometry can be immediately read from the asymmetric units.

The known structure of  $RbSb_3S_5 \cdot H_2O$  (6) is similar to that of  $[(CH_3NH_3)_{1.03}K_{2.97}]Sb_{12}S_{20} \cdot 1.34H_2O$ .  $RbSb_3S_5 \cdot H_2O$  has a chain structure if only strong Sb-S bonds shorter than 2.62 Å are considered. However, the chains are interconnected by secondary Sb-S bonds into two-atom-thick layers, as shown in Fig. 7a. By using the symbol scheme described above, the layer can be represented as shown in Fig. 7c. Every row and every column have the line group symmetry  $\bar{1}$ , and asymmetric units  $\uparrow\downarrow\uparrow\downarrow\uparrow$  and  $\uparrow\downarrow\uparrow\downarrow$  respectively. Both are different from those of the layer in the title compound. Theoretically there are six types of possible 5-atom-positions long asymmetric units corresponding to the stoichiometry of  $Sb_3S_5$ : (a)  $\uparrow\downarrow\uparrow\downarrow\uparrow$ ; (b)  $\uparrow\downarrow\uparrow\downarrow\downarrow$ ; (c)  $\uparrow\downarrow\uparrow\downarrow\uparrow$ ; (d)  $\uparrow\downarrow\uparrow\downarrow\downarrow$ ; (e)  $\downarrow\uparrow\downarrow\uparrow\downarrow$ ; (f)  $\uparrow\downarrow\uparrow\downarrow\uparrow$ . Four of them are found in the two structures discussed above ( $\uparrow\downarrow\uparrow\downarrow\uparrow\downarrow\uparrow\downarrow$  may be considered as  $\uparrow\downarrow\uparrow\downarrow\uparrow + \downarrow\uparrow\downarrow\uparrow\downarrow$ ). Many interesting hypothetical layer structures can be constructed from these units. Some of them also contain the 8-membered rings found in the structure of  $[(CH_3NH_3)_{1.03}K_{2.97}]Sb_{12}S_{20} \cdot 1.34H_2O$  which are marked in Fig. 6c and Fig. 7c. The two-atom-thick

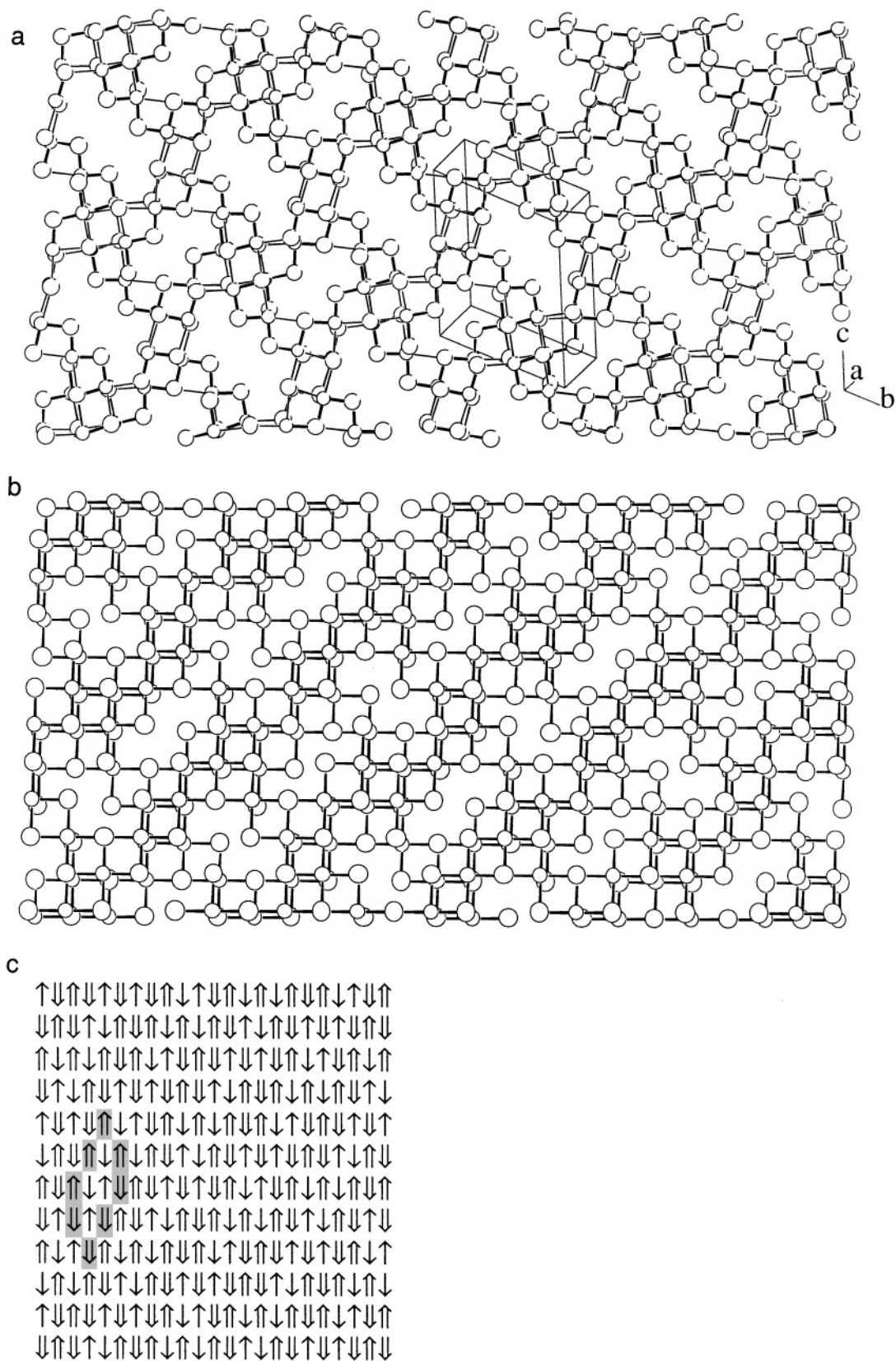


**FIG. 6.** Two-atom-thick layers in the structure of  $[(\text{CH}_3\text{NH}_3)_{1.03}\text{K}_{2.97}]\text{Sb}_{12}\text{S}_{20} \cdot 1.34\text{H}_2\text{O}$ , (a) viewed approximately perpendicular to the layers (large and small circles represent S and Sb atoms, respectively); (b) idealized pattern as NaCl structure derivative; and (c) the corresponding 2-dimensional net. An 8-membered ring is marked by shading.

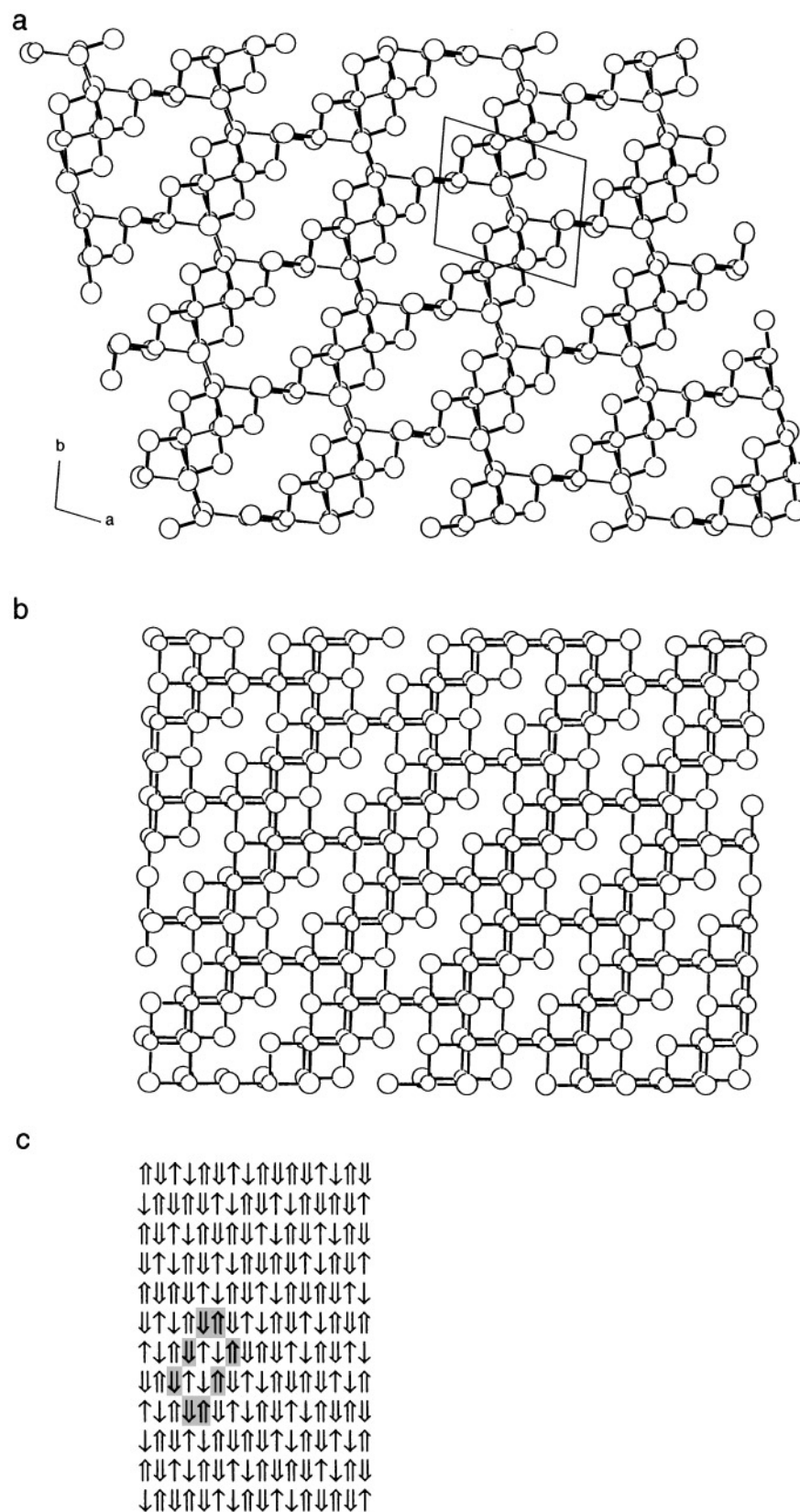


**FIG. 7.** Two-atom-thick layers in the structure of  $\text{RbSb}_3\text{S}_5 \cdot \text{H}_2\text{O}$  (6), (a) viewed approximately perpendicular to the layers (large and small circles represent S and Sb atoms respectively); (b) idealized pattern as NaCl structure derivative; (c) the corresponding 2-dimensional net. An 8-membered ring is marked by shading.

layers are also found in thioantimonates(III) with other stoichiometries such as  $\text{K}_2\text{Sb}_4\text{S}_7 \cdot \text{H}_2\text{O}$  (7) and  $[\text{C}_4\text{H}_{10}\text{N}]_2[\text{Sb}_8\text{S}_{13}] \cdot 0.15\text{H}_2\text{O}$  (16). Systematic exploration of possible layer topologies corresponding to different stoichiometries, combined with chemical considerations such as bond valence requirements may help to understand structural relations between known compounds of this type and design new ones. Our work along such directions is currently in progress.

#### ACKNOWLEDGMENTS

We thank the National Science Foundation (DMR9214804), the R. A. Welch Foundation, and the Deutsche Forschungsgemeinschaft for financial support. This work made use of MRSEC/TCSUH Shared Experimental Facilities supported by the National Science Foundation under Award Number DMR-9632667 and the Texas Center for Superconductivity at the University of Houston.

#### REFERENCES

- H. A. Graf and H. Schäfer, *Z. Anorg. Allg. Chem.* **414**, 211 (1975).
- H. A. Graf and H. Schäfer, *Z. Anorg. Allg. Chem.* **414**, 220 (1975).
- G. Dittmar and H. Schäfer, *Z. Anorg. Allg. Chem.* **437**, 183 (1977).
- K. Volk and H. Schäfer, *Z. Naturforsch. B* **33**, 827 (1978).
- G. Dittmar and H. Schäfer, *Z. Anorg. Allg. Chem.*, **441**, 98 (1978).
- K. Volk and H. Schäfer, *Z. Naturforsch. B* **34**, 172 (1979).
- B. Eisenmann and H. Schäfer, *Z. Naturforsch. B* **34**, 383 (1979).
- A. S. Kanishcheva, Yu. N. Mikhailov, V. G. Kuznetsov, and V. N. Batog, *Sov. Phys. Dokl.* **25**, 154 (1980).
- W. S. Sheldrick and H.-J. Häusler, *Z. Anorg. Allg. Chem.* **557**, 105 (1988).
- W. S. Sheldrick and H.-J. Häusler, *Z. Anorg. Allg. Chem.* **561**, 149 (1988).
- J. B. Parise, *Science* **251**, 293–294 (1991).
- J. B. Parise and Y. Ko, *Chem. Mater.* **4**, 1446 (1992).
- K. Tan, Y. Ko, and J. B. Parise, *Acta Crystallogr., Sect. C* **50**, 1439 (1994).
- X. Wang and F. Liebau, *J. Solid State Chem.* **385** (1994).
- X. Wang, *Eur. J. Solid State Inorg. Chem.* **32**, 303 (1995).
- Y. Ko, K. Tan, J. B. Parise, and A. Darovsky, *Chem. Mater.* **8**, 493 (1996).
- K. Tan, Y. Ko, J. B. Parise, J.-H. Park, and A. Darovsky, *A. Chem. Mater.* **8**, 2510 (1996).
- W. Bensch and M. Schur, *Eur. J. Solid State Inorg. Chem.* 1149 (1996).
- H.-O. Stephan and M. G. Kanatzidis, *J. Am. Chem. Soc.* **118**, 12226 (1996).
- W. S. Sheldrick and M. Wachhold, *Angew. Chem, Int. Ed. Engl.* **36**, 206 (1997).
- X. Wang and F. Liebau, "AICHe 1994 Annual meeting—Book of Extended Abstracts," p. 370. AICHe, 1994.
- J. B. Parise, K. Tan, P. Norby, Y. Ko, and C. Cahill, *Mater. Res. Soc. Symp. Proc.* **453**, 103 (1997).
- Siemens Analytical X-ray Instruments, SAINT, Version 4.05. Madison, WI, 1995.
- G. M. Sheldrick, SHELXTL, Version 5.03. Siemens Analytical X-ray Instruments, Madison, WI, 1995.
- N. Brese and M. O'Keeffe, *Acta Crystallogr., Sect. B* **47**, 192 (1991).
- X. Wang and F. Liebau, *Acta Crystallogr., Sect. B* **52**, 7 (1996).
- X. Wang and F. Liebau, *Z. Kristallogr.* **211**, 437 (1996).